IOP Publishing J. Neural Eng. 18 (2021) 046017 https://doi.org/10.1088/1741-2552/abed82

Journal of Neural Engineering

PAPER

RECEIVED
24 November 2020

REVISED
15 February 2021

ACCEPTED FOR PUBLICATION
10 March 2021

PUBLISHED
30 March 2021

Quantifying a frequency modulation response biomarker in responsive neurostimulation

Praveen Venkatesh[1], Daniel Sneider[1,5], Mohammed Danish[1,5], Nathaniel D Sisterson[2], Naoir Zaher[3], Alexandra Urban[3], Pulkit Grover[1], R Mark Richardson[2,4,*] and Vasileios Kokkinos[2,4]

[1] Department of Electrical and Computer Engineering, Carnegie Mellon University, Pittsburgh, PA, United States of America
[2] Department of Neurosurgery, Massachusetts General Hospital, 55 Fruit Street, Boston, MA 02114, United States of America
[3] Department of Neurology, University of Pittsburgh, Pittsburgh, PA, United States of America
[4] Harvard Medical School, Boston, MA, United States of America
[5] The authors contributed equally to this work.
[*] Author to whom any correspondence should be addressed.

E-mail: mark.richardson@mgh.harvard.edu

Keywords: epilepsy, epilepsy surgery, responsive neurostimulation, ictal frequency modulation, earth mover's distance

Abstract

Objective. Responsive neurostimulation (RNS) is an effective treatment for controlling seizures in patients with drug-resistant focal epilepsy who are not suitable candidates for resection surgery. A lack of tools for detecting and characterizing potential response biomarkers, however, contributes to a limited understanding of mechanisms by which RNS improves seizure control. We developed a method to quantify ictal frequency modulation, previously identified as a biomarker of clinical responsiveness to RNS. *Approach.* Frequency modulation is characterized by shifts in power across spectral bands during ictal events, over several months of neurostimulation. This effect was quantified by partitioning each seizure pattern into segments with distinct spectral content and measuring the extent of change from the baseline distribution of spectral content using the squared earth mover's distance. *Main results.* We analyzed intracranial electroencephalography data from 13 patients who received RNS therapy, six of whom exhibited frequency modulation on expert evaluation. Patients in the frequency modulation group had, on average, significantly larger and more sustained changes in their squared earth mover's distances ($\text{mean} = 13.97 \times 10^{-3} \pm 1.197 \times 10^{-3}$). In contrast, those patients without expert-identified frequency modulation exhibited statistically insignificant or negligible distances ($\text{mean} = 4.994 \times 10^{-3} \pm 0.732 \times 10^{-3}$). *Significance.* This method is the first step towards a quantitative, feedback-driven system for systematically optimizing RNS stimulation parameters, with an ultimate goal of truly personalized closed-loop therapy for epilepsy.

1. Introduction

The responsive neurostimulation (RNS) system is a closed-loop brain stimulation system, FDA-approved as an alternative treatment for drug-refractory focal epilepsy patients, who are not considered suitable candidates for resective surgery. The responsive neurostimulator automatically analyzes the intracranial electroencephalogram (iEEG), detects seizures and rapidly delivers electrical stimulation to suppress seizure activity (Kossof *et al* 2004). Studies of class 1 evidence have reported 44% seizure reduction at one year post-implantation, 53% at two years (Heck *et al* 2014), and a 48%–66% reduction in seizure occurrence between the third and sixth post-implantation years in open-label continuation studies (Bergey *et al* 2015). A median 70% of patients with both mesiotemporal and neocortical seizure onset experienced significant reduction in seizure frequency at six years post-implantation, 26%–29% benefited from a post-implantation seizure-free period of at least six months and 15% experienced one year or longer free from seizures (Geller *et al* 2017, Jobst *et al* 2017). A more recent retrospective study reported a median reduction of 67% in seizures at one year, 75% at two years, 82% at

⩾three years and 74% at the most recent follow-up (Razavi *et al* 2020). A prospective open label trial to evaluate RNS efficacy found a median 75% of patients experienced seizure reduction at nine years post-implantation, and 35% of patients had ⩾90% reduction in seizure frequency (Nair *et al* 2020). These results compare favorably to alternate neuromodulation strategies such as vagal nerve stimulation and deep brain stimulation (Sisterson and Kokkinos 2020).

Although the RNS system has been shown to provide improved seizure control and quality of life in patients with pharmaco-resistant focal epilepsy, its mechanisms of action are still under investigation. Historically, the primary hypothesis has been that patients experience a decreased seizure burden as a result of direct inhibition of ongoing ictal activity by electrical stimulation (Lesser *et al* 1999, Kossoff *et al* 2004, Skarpaas and Morrell 2009, Morrell and Halpern 2016). Although isolated samples of recordings and corresponding spectrograms supporting this hypothesis have been presented sporadically in the literature (Skarpaas and Morrell 2009, Thomas and Jobst 2015, Geller *et al* 2017, Jobst *et al* 2017), no systematic studies have presented an in-depth analysis of the brain's response to closed-loop stimulation events. We recently tested the hypothesis of whether clinical efficacy arises from successful detection-triggered electrical stimulation and subsequent instantaneous, or 'direct', termination of seizure activity, and instead found evidence for an altogether different therapeutic mechanism involving chronic, or 'indirect', effects (Kokkinos *et al* 2019). In this prior work, we evaluated time and time-frequency features beyond a narrow direct stimulation interval, throughout the time course of the iEEG recordings, and discovered discrete categories of 'indirect' modulation effects, which appeared independent of acute stimulation events and were associated with improved clinical outcomes. In contrast, detection-triggered 'direct' stimulation effects were not associated with responsiveness to RNS therapy. In effect, this study established several key biomarkers of a patient's responsiveness to RNS therapy, characterized by reduced seizure frequency, severity and/or duration. The identification of these biomarkers suggested that chronic responsive stimulation progressively disrupts the connectivity of the epileptogenic network and reduces the core synchronized population strength.

This prior work was largely *qualitative*, demonstrating visually appreciable changes in time and frequency domains, similar to clinical observational practice, and without a strong quantitative backbone. In the current study, we take a step further and develop a *quantitative* metric for describing one specific iEEG response biomarker established by Kokkinos *et al* (2019): the ictal frequency modulation effect.

2. Methods

Our main contribution is a technique for quantifying the extent of *indirect frequency modulation* in the seizures of a patient, an effect that was characterized by a shift in spectral energy across frequency bands over several months of RNS stimulation (see Kokkinos *et al* 2019). Quantifying the shift in spectral energy over multiple months was made challenging by a few factors: (a) the diversity of spectral content *within* each seizure of a patient had to be *discounted*, while changes in spectral content *across* seizures had to be *accounted* for; (b) if a patient had two or more 'types' of seizures, short-term differences had to be discounted, while long-term changes had to be accounted for; and (c) the method had to handle a broad diversity of time-frequency patterns seen across multiple patients.

To handle these requirements, we converged on a method that first captured the spectral diversity within seizures in a short time period, and then quantified frequency modulation across seizures over a longer time period. The short-term spectral diversity was represented using a *distribution of vectors* in three-dimensional (3D) space, and frequency modulation was quantified over a longer time period using a *distance between these distributions*. Our method consisted of two main stages: (a) partitioning seizures into segments based on their frequency content (described further in section 2.3); and (b) constructing distributions from these segments and measuring distances between distributions to quantify frequency modulation (described further in section 2.4).

2.1. Patients and data

Data were obtained from an IRB-approved database of all epilepsy surgeries performed in a single surgeon practice at the University of Pittsburgh Medical Center (Pittsburgh, PA, USA). All patients were diagnosed with refractory focal epilepsy according to current ILAE criteria (Berg *et al* 2010, Fisher *et al* 2017) and chronically implanted with closed-loop neurostimulation (RNS System, NeuroPace, Mountain View, CA, USA) after consensus recommendation in a multidisciplinary epilepsy patient management conference. Data from 13 consecutive patients implanted with the RNS system between January 2015 and June 2018 were included in this study.

All patients had either neocortical or hippocampal implantation (table 1), with two leads. Immediately post-implantation, the device was set to passive recording mode for approximately one month (on average, across patients) during which no stimulation was delivered; we call this period the *baseline epoch*. Once the baseline activity was reviewed, stimulation parameters were configured and activated by the clinical team. In turn, detection-triggered stimulation therapy parameters were periodically modified in subsequent clinic visits, based on a clinical

Table 1. Patient data.

Patient	Age	Gender	Implantation sites	Postop months	# Seizure patterns	Frequency modulation effects	Outcome (Engel scale)
1	29	M	Cortical malformation	24	29	Indirect	IIB
2	22	M	Neocortex	29	22	Indirect	IIB
3	39	F	Cortical malformation	36	2032	Indirect	IIIA
4	24	M	Neocortex	22	92	Indirect	IIIA
5	34	F	Neocortex	46	430	Indirect	IB
6	42	F	Neocortex	49	823	Direct	IVB
7	22	F	Hippocampus	43	487	None	IVB
8	47	F	Cortical malformation	53	263	None	IIIA
9	37	M	Neocortex	52	20	None	IIA
10	22	F	Hippocampus	42	1013	None	IVA
11	30	M	Hippocampus	16	48	None	IA
12	39	F	Hippocampus	30	141	None	IVB
13	63	F	Neocortex	51	2072	None	IB

evaluation of seizure control status. The time intervals between RNS parameter modifications, during which both detection and stimulation settings remained unchanged, are referred to as programming epochs.

iEEG recordings and additional metadata, including recording and detection settings, were retrieved from the NeuroPace Patient Data Management System (PDMS) using automated in-house custom-built software (Sisterson *et al* 2019). All recordings were 90 s periods of four-channel iEEG, online band-pass filtered at 4–125 Hz, sampled at 250 Hz, and digitized by a 10 bit ADC. iEEG channels were recorded in a bipolar montage between neighboring electrode contacts, with the case of the RNS pulse generator acting as the amplifier ground. All electrode impedances measured below 1 kΩ during regular post-implantation clinical visits.

iEEG seizure pattern onsets were annotated based on visual evaluations conducted independently by an experienced epilepsy surgery neurophysiologist (VK) and a board-certified epileptologist (NZ). Inter-rater agreement on whether each 90 s snippet of data contained a seizure pattern was 99.8%. iEEG seizure pattern onset was defined as the point in time after which the iEEG background was no longer interictal and was followed by paroxysmal discharges with ictal features and morphology developing over time. The interictal background, both in the awake and sleep states, was appreciated from scheduled recordings and iEEGs that did not contain seizure patterns.

2.2. Preprocessing

The data corresponding to each programming epoch were comprised of a number of distinct files containing 90 s of continuous iEEG data. These files were not always contiguous and therefore were processed independently of each other. Only seizure patterns that had an onset within a file were considered; seizure patterns for which the onset was not captured were discarded. For each seizure pattern, only the recording period between the onset and the end of the respective iEEG file was considered for analysis.

Beyond the baseline epoch, therapeutic neurostimulation was active for all epochs. Stimulation intervals appeared in the iEEG recording as an artifact, characterized by a flat signal, followed by a brief increase with an exponential decay. To remove this artifact, we searched for segments of iEEG data that were constant for at least 250 ms across all channels and then eliminated these segments. We also fit an exponential curve to identify the subsequent burst, and disregarded data until it fell to 5% of the peak of the burst.

2.3. Processing: spectral content-based partitioning of seizure patterns

We first used an algorithm to temporally partition each seizure pattern into segments based on their spectral content. This step played the important role of isolating segments with distinct spectral content from their neighbors, so as to concisely represent the diversity in frequency content of a single seizure using a small number of segments. This process was essential for decreasing the computational burden associated with quantifying differences in frequency content across many seizures over long time periods.

For each patient, a single RNS channel was designated the *onset channel* by visual inspection (figure 1(a)). This channel was used for all subsequent analyses for that patient. The partitioning of iEEG seizure patterns comprised five discrete steps:

(1) For each seizure pattern, we computed the short-time Fourier transform (STFT), also known as the spectrogram, using a 1 s wide Kaiser window ($\beta = 10$) and a step size of 62.5 ms (figure 1(b)).
(2) The spectrogram was thresholded using a 1 s wide moving window at steps of 0.25 s. In each window, we hard-thresholded (e.g. see Mallat

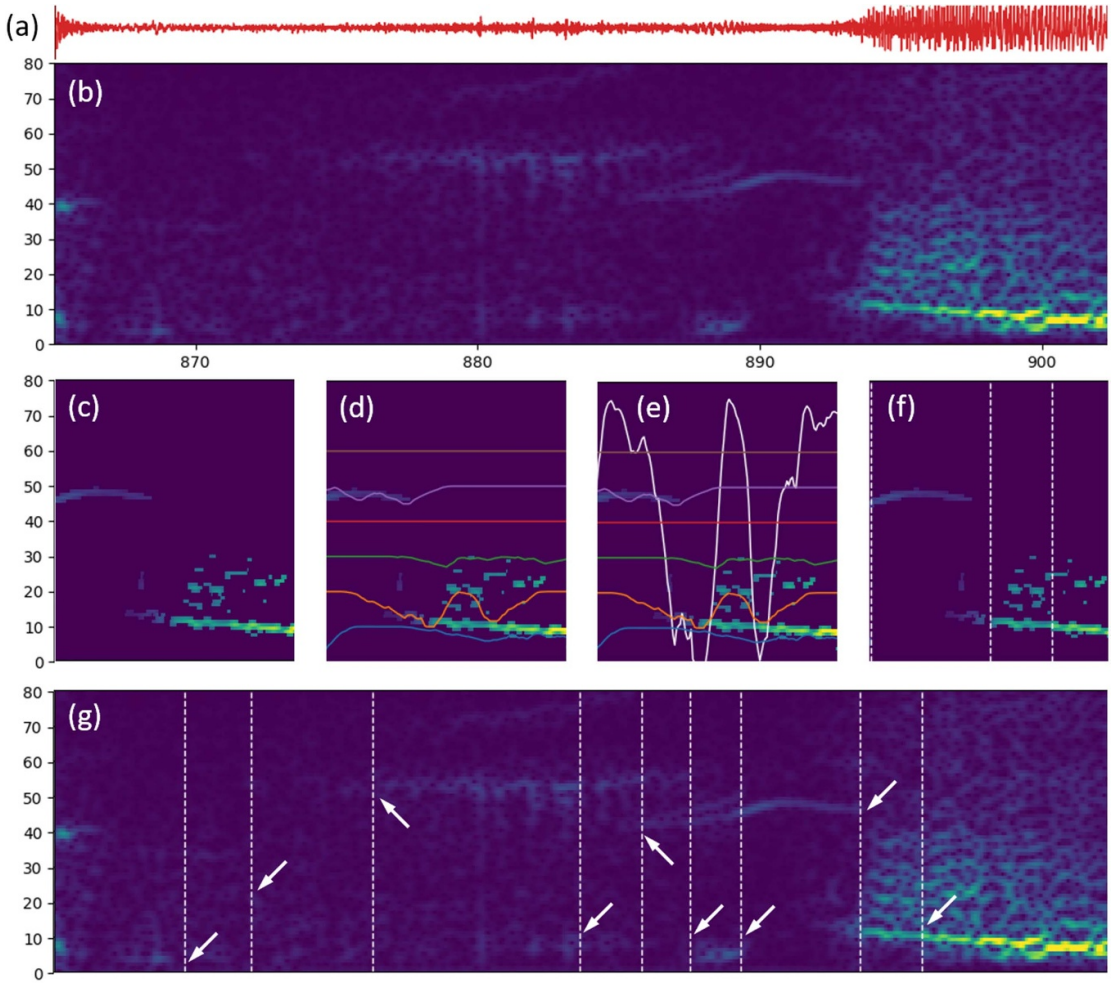

Figure 1. A depiction of the process of seizure partitioning. (a) Data from a single iEEG channel, here, the first 35 s of a typical seizure from patient 7 is shown for illustration. (b) The STFT of the aforementioned time-domain data. Only frequencies from 0 to 60 Hz are used in the analysis. (c) STFT snippet after thresholding has been applied. (d) KS-test p-values for change detection superimposed upon the STFT snippet: each colored line represents log-scaled p-values for KS tests conducted for a 10 Hz wide frequency bin. For example, the orange line represents the 10–20 Hz bin with the y-axis is scaled as follows: 20 Hz corresponds to a p-value of 1, while 10 Hz corresponds to a p-value of 10^{-8}. The other lines are shifted according to their respective frequency bin and are scaled similarly. (e) The Fisher-combined p-value (after log-scaling) superimposed in white, with the y-axis scaled as follows: 80 Hz corresponds to a combined p-value of 1, while 0 Hz corresponds to a combined p-value of 10^{-8}. (f) Peak detection applied to the combined p-values to detect change points, shown by white dashed vertical lines. (g) All change points for the first 35 s of this seizure: note how points at which the seizure frequency content changes (indicated by white arrows) are correctly identified as change-points (indicated using vertical white dashed lines) that are used to define separate segments.

2009) all frequency values that had an amplitude less than half the peak amplitude within that window (figure 1(c)).

(3) We then analyzed the spectrogram for change points at intervals of 0.05 s. For each putative change point, we compared the 2 s window before that time instant to the 2 s window following it. These two windows were compared for six distinct frequency bins (each 10 Hz wide, spanning 0–60 Hz). For each frequency bin, we performed a two-sample Kolmogorov–Smirnov (KS) test (Kass *et al* 2014) to assess whether the distribution of frequency magnitudes in the two windows differed significantly. Accordingly, we computed six different p-values of the KS test for each frequency bin (figure 1(d)).

(4) The p-values were combined across bins using Fisher's method to produce a single aggregate p-value at each tested time instant. It should be noted that this is not a statistically rigorous use of Fisher's method, since the p-values being combined are, in general, not independent. However, this was found to be a reasonable heuristic for the purposes of segmentation (figure 1(e)).

(5) Finally, change points were declared using a peak-detection algorithm (Virtanen *et al* 2020) on the negative logarithm of the aggregate p-values. We set the 'prominence' parameter (minimum height from base-to-peak) of our peak detection algorithm to 'two units', which had the effect of identifying distinct, well-separated peaks while ensuring that only

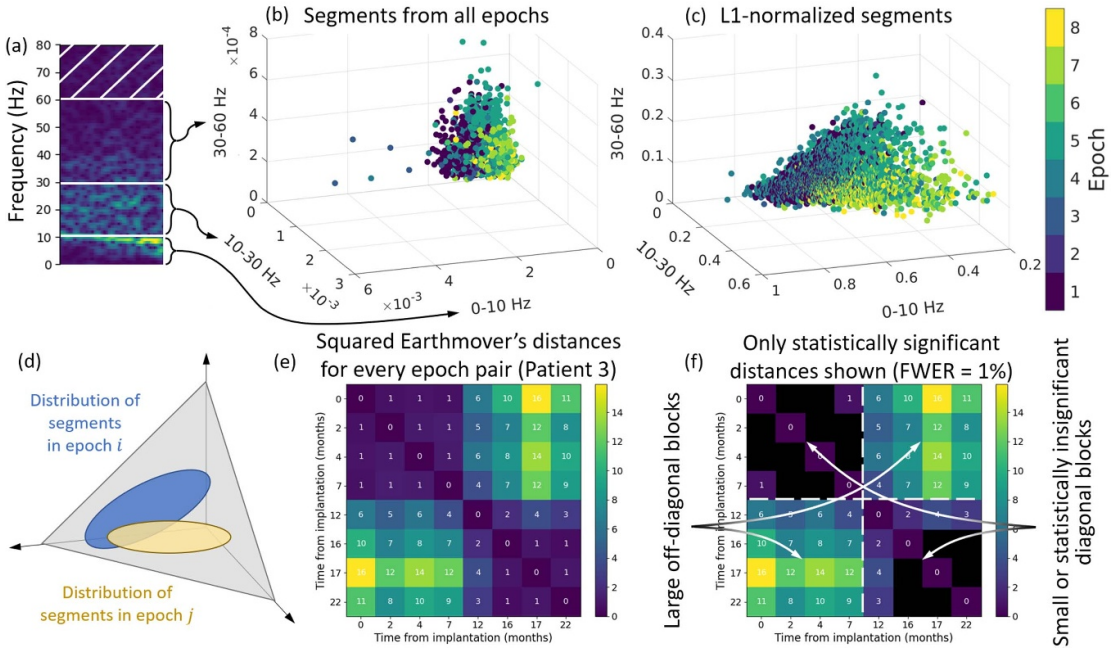

Figure 2. A depiction of the process of quantifying frequency modulation in a patient. (a) Each seizure segment is divided into three frequency bins: 0–10 Hz, 10–30 Hz and 30–60 Hz (frequencies greater than 60 Hz were discarded). The average frequency magnitude in each of these bins is the value on each of the axes of the 3D image in (b); each seizure segment is thus condensed to a single point. Figure (b) shows segments from all seizures across all epochs; the color of each segment represents the index of the programming epoch it appears in (data from patient 3 shown for illustration). (c) Seizure segments normalized to have unit L1-norm. (d) A caricature of the distributions of segments from two different epochs; the squared earth mover's distance is computed between every such pair of empirical distributions, as shown in (e). Significance is evaluated using a permutation test and we report only those distances significant at a family-wise error rate of 1% (for each patient), shown in (f); statistically insignificant distances are represented by black squares. Also seen in (f) is a clear representation of the 'block-matrix' structure that is typical in patients who show indirect frequency modulation: the dashed lines indicate how the matrix may be roughly divided into four rectangular 'blocks' of cells. Note that the two blocks along the diagonal of the matrix ('diagonal blocks') appear dark, having small or statistically insignificant distances, while the two remaining 'off-diagonal' blocks appear bright, having large statistically significant distances.

p-values less than 10^{-2} were selected (figures 1(f) and (g)).

Of these steps, the segmentation algorithm was found to be particularly sensitive to the length of the thresholding window and the value of the threshold. Other parameters did not affect the segmentation output considerably.

2.4. Processing: quantification of frequency modulation in seizure patterns

Having partitioned each seizure pattern into segments based on frequency content, we proceeded to use these segments as features for quantifying frequency modulation in each patient. This process consisted of seven discrete steps:

(1) Considering only frequencies from 0 to 60 Hz, we first condensed each segment into a 3D vector, comprising the average frequency magnitude in three different frequency bands: 0–10 Hz, 10–30 Hz and 30–60 Hz (figures 2(a) and (b)).
(2) Since each patient had different RNS signal amplitudes, we normalized each vector by the sum of its components (also called the vector's L1-norm; see figure 2(c)). This had the effect of balancing signal energies across each patient's epochs, as well as across all patients, providing a common platform to compare the extent of frequency modulation. Note that this step further condensed each segment to a two-dimensional (2D) vector lying on the standard simplex (figure 2(d)).
(3) We then grouped all segments arising from seizure patterns within a given programming epoch (indicated by colors in figures 2(b) and (c)). Our quantification of frequency modulation depended only on the statistics of these segments across epochs. This strategy ensured that we could reliably capture indirect frequency modulation effects that were a result of chronic stimulation, while reducing the likelihood of capturing direct frequency modulation effects that were an instantaneous result of stimulation.
(4) For each programming epoch, we computed the *weighted empirical distribution* of segments on the standard 2D simplex (figure 2(d)). This empirical distribution was simply a collection of point masses at every segment's vector,

normalized by the total number of segments in that epoch. Weights were assigned to each segment based on the time-length of each seizure segment. The weighted empirical distributions, therefore, captured the extent of variation in frequency amplitudes (weighted by duration) across all seizure patterns within each programming epoch.

(5) The extent of frequency modulation between two epochs was quantified using a squared earth mover's distance (also called the Wasserstein distance; Villani 2008) between their corresponding empirical distributions (figure 2(e)). Intuitively, if we visualize these distributions as mounds of earth, then the squared earth mover's distance quantifies the minimum amount of 'work' (~mass times distance) needed to rearrange the earth of one distribution so as to make into the other (for a detailed mathematical definition, see Villani 2008). We computed this distance using an optimal transport algorithm (Flamary and Courty 2017).

(6) Finally, for every pair of epochs, we tested whether the computed distance was significantly different from zero by using a permutation test (Kass *et al* 2014). We constructed an empirical null distribution by randomly permuting segments between the two epochs 10 000 times (keeping the number of segments in each epoch fixed) and computing the squared earth mover's distance between the resulting weighted empirical distributions each time. The estimated p-value was then the probability, under the empirical null distribution, of exceeding the true squared earth mover's distance (which was computed on the non-permuted data).

(7) Since we have multiple hypothesis tests for each patient, we identified all pairwise squared earth mover's distances that were significant at a *family-wise error rate* of 0.01 for each patient using Bonferroni's method (Kass *et al* 2014). This is equivalent to performing a Bonferroni correction against the number of pairwise comparisons for each patient (figure 2(f)).

2.5. Patient outcomes

Seizure outcomes were derived by personal impact of epilepsy scale (PIES) questionnaires (Fisher *et al* 2015). PIES questionnaires were supplemented with three queries regarding seizure manifestation: (a) the estimated mean frequency of seizure occurrence before and after RNS implantation, per month in absolute numbers; (b) the estimated mean severity of seizures, on a scale of 1–5 (1: not severe, 5: very severe); and (c) the mean duration of seizures, in minutes. We used the Engel classification (Engel *et al* 1993) to group our patients as either responders (Engel class III or better) or non-responders (Engel class IV), based on the scores of the three seizure manifestation variables (see table 1).

3. Results

We analyzed data from 13 patients implanted with the RNS system (five male, mean age = 34 years, age range 22–63). The mean time after implantation to activation of responsive stimulation was six weeks (SD: 3.6). A total of 23 868 iEEG files were visually reviewed, corresponding to 316 months of post-surgical implantation recordings spanning a 41 month total study period. A total of 7472 seizure patterns were identified. After analysis presented in our prior work (Kokkinos *et al* 2019) and extended in this cohort of patients, both direct and indirect ictal frequency modulation was appreciated in six of our patients (patients 1 through 6), while the remaining seven (patients 7 through 13) did not demonstrate any visually appreciable change in ictal frequency content. For judging whether patients exhibited indirect frequency modulation, we relied on the evaluation criteria proposed in our earlier work (Kokkinos *et al* 2019).

For each patient's recordings, we measured the extent of frequency modulation between every pair of programming epochs by using a squared earth mover's distance between the weighted empirical distributions of the epochs' seizure segments. Recordings from patients in the expert-identified frequency modulation group, on average, exhibited larger magnitudes of squared earth mover's distances (mean $= 13.97 \times 10^{-3} \pm 1.197 \times 10^{-3}$ among statistically significant values reported in figures 3 and 4 combined, for patients 1–6; mean $= 14.49 \times 10^{-3} \pm 1.282 \times 10^{-3}$ among statistically significant values reported in figure 3 alone, for patients 3–6) than recordings from patients who did not show frequency modulation in the visual examination (mean $= 4.994 \times 10^{-3} \pm 0.732 \times 10^{-3}$ among statistically significant values reported in figure 5 for patients 7–13).

Analysis of recordings in the expert-identified frequency modulation group produced squared earth mover's distance matrices with a *block-matrix structure*, with larger distances in off-diagonal blocks and distances close to zero on diagonal blocks (see figure 2(f) for an illustration of 'block-matrix structure' and figure 3 for results). These recordings followed a pattern: squared earth mover's distances show a marked increase after a specific programming epoch that was subsequently sustained. This finding is represented by a visually distinct block-matrix structure: diagonal blocks appear dark, having either very small or statistically insignificant distances, while off-diagonal blocks are bright, indicating a sustained change in the frequency content of these patients' seizure patterns (as illustrated in figure 2(f)). For example, in patient 3, the squared earth mover's

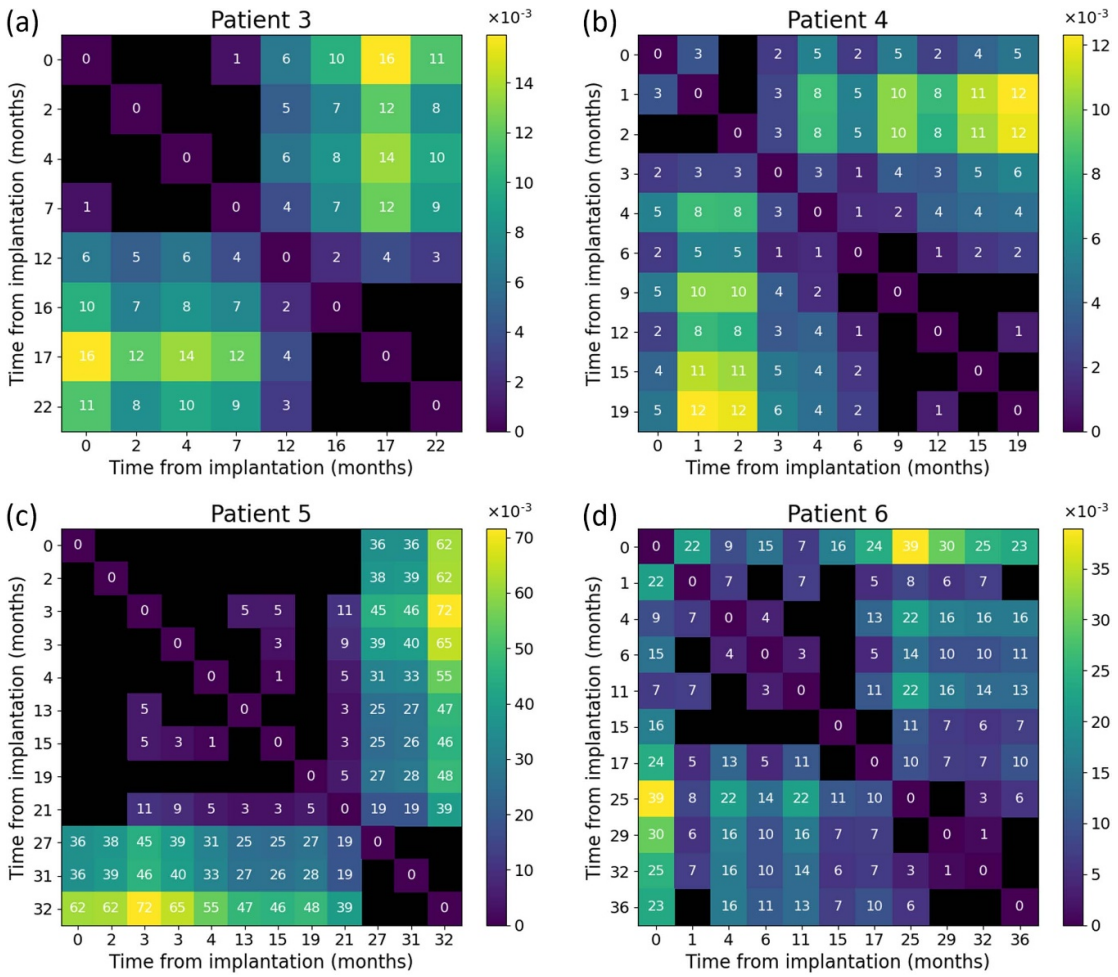

Figure 3. Squared earth mover's distances between every pair of programming epochs, in patients who showed indirect frequency modulation according to an expert visual evaluation. Note that '0' refers to the baseline epoch, while blacked-out squares represent distances that were not statistically significant at a family-wise error rate of 1% for each patient.

distance from the baseline epoch remains close to zero (or indistinguishable from zero) for the first 12 months after implantation; subsequently it rises to an average value of 10.75×10^{-3} over the next 10 months (figure 3(a)). Similarly, recordings from patient 5 showed squared earth mover's distances indistinguishable from zero until the 27th month post-implantation, after which it rises in the last three epochs, attaining a maximum of 72×10^{-3} (the largest distance observed within our cohort) (figure 3(c)). Although recordings from patient 6 were classified as showing direct frequency modulation in the expert evaluation, our method (which was designed primarily for indirect frequency modulation) demonstrated large, statistically significant changes in squared earth mover's distance, as well as a visually apparent block-matrix structure. This suggests that our method may be sensitive to both indirect and direct frequency modulation effects.

The squared earth mover's distances of patients 3 through 6 does not always increase smoothly or even monotonically across epochs. Since RNS stimulation parameters were tuned between epochs, we believe that such fluctuations result from a combination of changes to these parameters and the effects of prolonged exposure to stimulation. As such, the indirect frequency modulation effect is best appreciated in the aggregate, e.g. in the block-matrix structure of the squared earth mover's distance matrices.

Patients 1 and 2 were assigned to the frequency modulation group in the expert analysis, however, the programming epochs that contributed most to frequency modulation had an insufficient number of seizure patterns to obtain statistically meaningful squared earth mover's distances (figure 4). Patient 1 had too few seizure events: 2, 18, 5, 4 and 9 events, respectively, in their five programming epochs (figures 4(a)–(c)). Patient 2 showed signs of frequency modulation, as is apparent from the block-matrix structure in the full matrix (figures 4(d)–(f)), but the epochs that appeared to show the largest modulation effects were also those with the smallest number of seizure episodes (the first five programming epochs had 2, 5, 12, 0 and 15 recorded seizure events; an epoch without seizure events was not included in the matrix). Thus, several distances did not pass

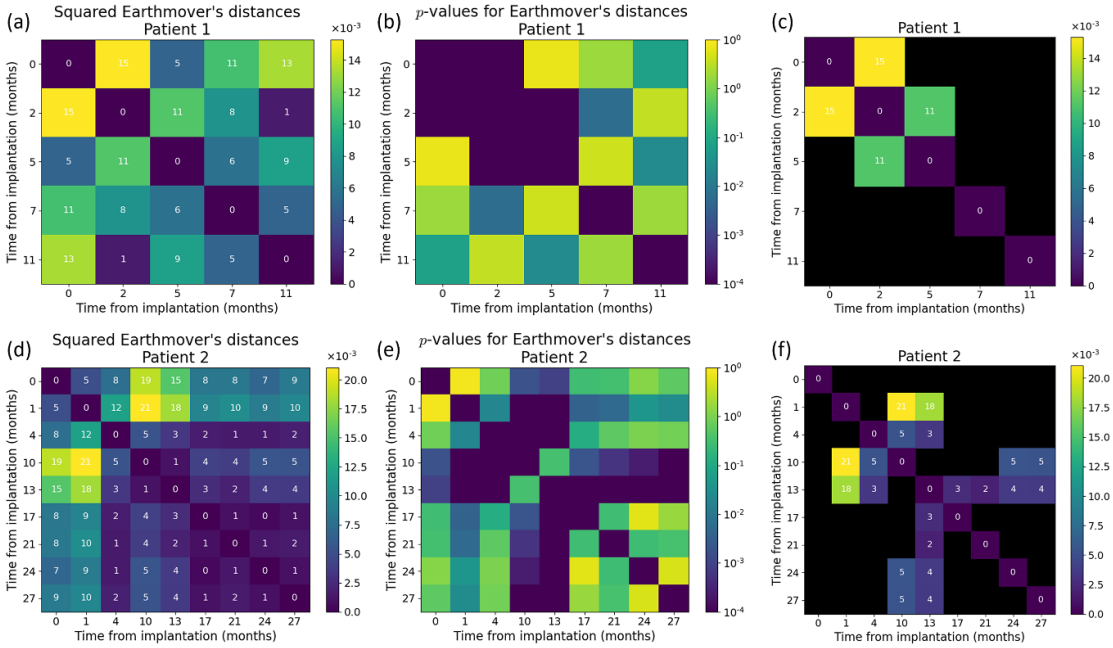

Figure 4. Results for patients 1 and 2, both of whom showed frequency modulation in an expert evaluation. (a)–(c) Patient 1 had too few seizures to be able to see frequency modulation when using our measure. (d)–(f) Patient 2 had too few seizures in the first few epochs, which is where the squared earth mover's distances are more pronounced. Thus, in both cases, the statistical significance of these distances could not be established.

the statistical threshold at a family-wise error rate of 0.01. Based on the data available to us, we find that our algorithm starts becoming effective when working with at least 15–20 seizure events per programming epoch and performs more reliably as the number of seizure patterns per programming epoch increases.

Recordings from the group without expert-identified ictal frequency modulation did not demonstrate a clear pattern of squared earth mover's distances change and often had distances that were either small or statistically insignificant (figure 5). For example, in recordings from patient 8, almost all squared earth mover's distances are statistically insignificant, the remaining few being small relative to those values from the group of patients who exhibited statistically significant frequency modulation. In the case of patient 7, most distances were significant, however they were all quite small ($<6 \times 10^{-3}$) and showed no clear block-matrix structure.

4. Discussion

Understanding the effects of RNS in any given epilepsy patient requires substantial effort by clinicians to manually review recorded electrocorticograms. As new potential biomarkers of clinical response are discovered, the burden on clinicians to recognize and quantify these electrophysiological responses will continuously increase. It is imperative, therefore, to develop tools to automate the process of response biomarker detection. In this study we described a method that could differentiate patients who were identified by experts as showing signatures of ictal frequency modulation, from patients who did not. The recordings of the former group exhibited squared earth mover's distance matrices with a block-matrix structure, with large distances in off-diagonal blocks and small or statistically insignificant distances in diagonal blocks. In contrast, recordings from the latter group exhibited no clear block-matrix structure, and often had squared earth mover's distances that were either uniformly low or statistically insignificant. We also found that the earth mover's assay for quantifying frequency modulation performed most reliably when the number of seizure events increased to at least 15–20 per programming epoch.

4.1. Implications for the mechanism of RNS

The efficacy of cortical electrical stimulation, and RNS in particular, in seizure control has been clearly demonstrated throughout the literature (Penfield and Jasper 1954, Velasco *et al* 2000, Yamamoto *et al* 2002, Kinoshita *et al* 2004, Kossoff *et al* 2004, Kinoshita *et al* 2005, Elisevich *et al* 2006, Yamamoto *et al* 2006, Stacey and Litt 2008, Velasco *et al* 2009, Child *et al* 2014, Heck *et al* 2014, Ludstrom *et al* 2016, 2017, Valentin *et al* 2016, Geller *et al* 2017, Jobst *et al* 2017, Kerezoudis *et al* 2017, Valentin *et al* 2017, Nair *et al* 2020, Razavi *et al* 2020, Sisterson *et al* 2020). However, apart from a few original publications (Lesser *et al* 1999, Kossoff *et al* 2004, Osorio *et al* 2005), little has been known about the electrographic manifestations of RNS therapy, or its mechanisms of action for reducing seizure severity and frequency, until recently.

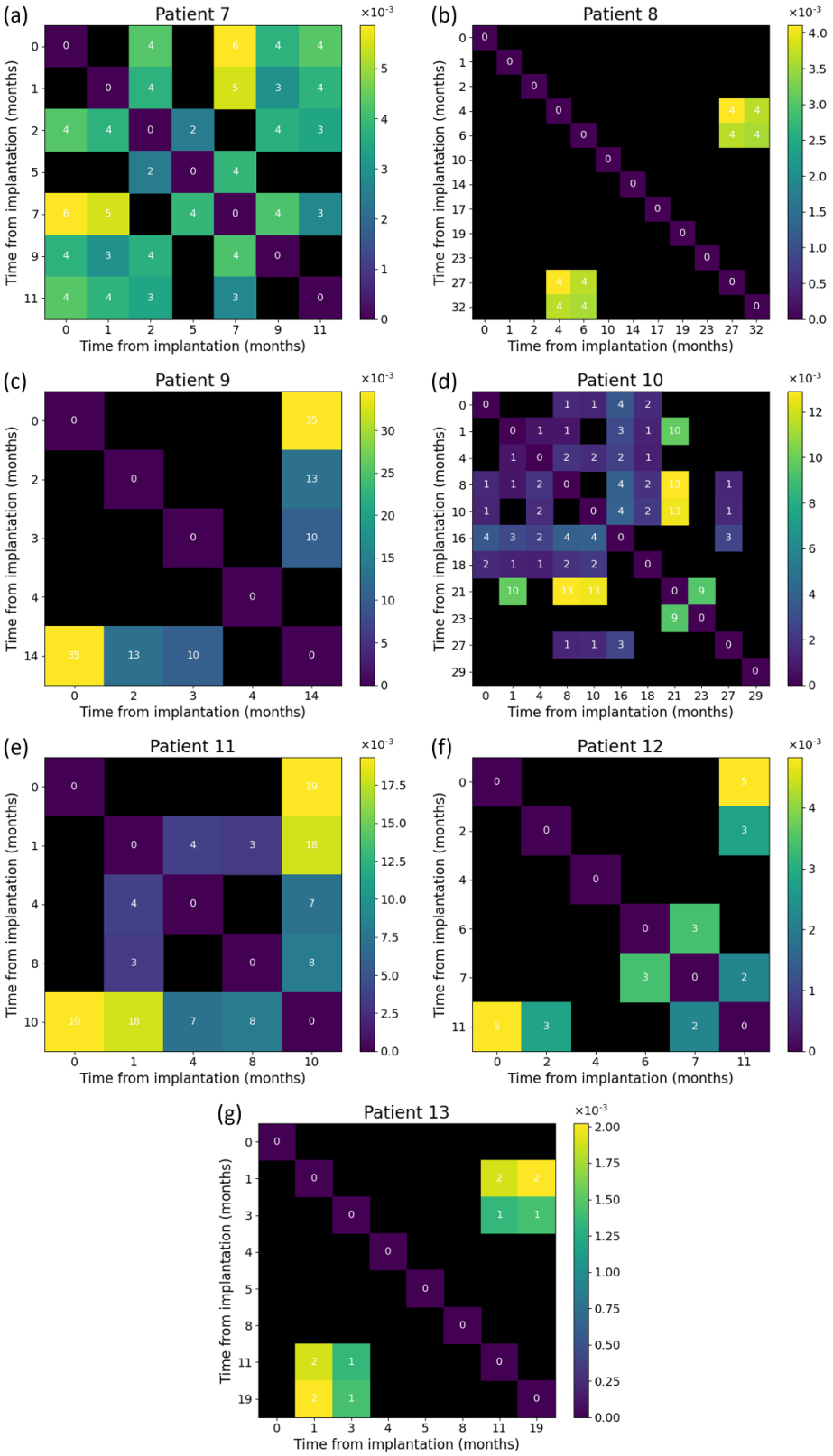

Figure 5. Squared earth mover's distances between every pair of programming epochs in patients who did not exhibit indirect frequency modulation effects according to an expert visual evaluation.

Previously, the mechanism was assumed to be direct, i.e. the interruption of ictal activity by stimulation close to the seizure focus (Kossoff *et al* 2004, Skarpaas and Morrell 2009, Morrell and Halpern 2016). However, a recent work of ours highlighted the existence of indirect modulation effects that correlated with responsiveness to RNS, thereby providing a novel paradigm for RNS's mechanism of action (Kokkinos *et al* 2019). In particular, the presence of frequency modulation effects among our earlier findings showed that parts of the underlying epileptogenic tissue can be progressively re-tuned by

stimulation to oscillate at different frequencies than before RNS. These findings were consistent with the reported increase of patient responsiveness over time (Bergey *et al* 2015, Razavi *et al* 2020).

Our initial study was largely qualitative, adhering to the principles of routine clinical evaluation of iEEG recordings. In the present study, we took one step further towards objectifying and quantifying our observations on ictal frequency modulation in RNS. Our automated quantitative approach enables a more in-depth, objective analysis RNS's mechanism of action on a larger patient cohort. Future work will examine the correlation between patients' subjective ratings of their outcomes (e.g. seizure frequency and severity) and the magnitude of indirect frequency modulation as measured using our earth mover's metric, on an epoch-by-epoch basis.

4.2. Alternative quantification approaches

Considering the complexity of our approach for quantifying frequency modulation, it is worth understanding which steps of our process are essential, and which may be dispensable.

The process of seizure partitioning, for instance, was carried out with a great deal of care, using a sophisticated statistical change-detection algorithm. On the one hand, it is not possible to do away with partitioning *entirely*: treating the seizure as one continuous segment and averaging the frequency content over the entire seizure would prevent us from detecting subtle changes not captured in the average, while treating every single time instant as a separate segment would place an impossibly high computational burden on the computation of earth mover's distances. However, it may be possible to achieve a similar result using segments having a uniform, fixed length of around 3–5 s. This would have the downside of capturing some segments that straddled periods with distinct frequency signatures, but this may not severely affect the final appraisal of the block-matrix nature of distance matrices. Since we have no ground truth knowledge of the 'true extent' of indirect modulation, an objective comparative analysis of different partitioning methods is infeasible. As such, we believe a well-calibrated change-detection approach is most likely to provide accurate results.

A potential avenue for future work is to better understand some of the specifics of our method, e.g. the method used to estimate the distribution of segments, the choice of distance measure, the number of frequency bins to consider and their ranges, etc. Such analyses might evaluate alternative approaches by comparing how well they correlate with clinical outcomes.

4.3. Implications for optimizing stimulation parameters

There are currently no patient-specific guidelines for optimal regulation of either detection or stimulation parameters for RNS (Sisterson *et al* 2019, 2020). Quantification of the frequency modulation biomarker described here, however, provides insight for understanding how this type of information might be used prospectively to optimize stimulation parameters. Take the example of data from non-responder patient 8 shown in figure 5(b), which did not demonstrate visually appreciable frequency modulation. The majority of programming epochs demonstrated no sign of frequency modulation. However, in programming epochs corresponding to months 4–6 post-implantation, statistically significant indications of frequency modulation appear. It is possible that the specific combination of detection and stimulation settings during that treatment phase had the potential to modulate the epileptogenic neuronal substrate and change the ictal oscillation frequency range, without rendering these changes visually appreciable. If the clinician had received this information at the time, settings might have been preserved and the patient's matrix might have developed like that of responder patient 5 in figure 3(c), who demonstrated frequency modulation effects only after 27 months post-implantation and a considerable number of changes in settings. Our results show that our method not only quantifies specific modulation effects but can also act as a pointer towards the optimal settings that provoke said neuromodulation effects. Analyses that correlate detection and stimulation settings with our earth mover's distance metric are ongoing and will be the subject of a subsequent study.

5. Conclusion

We developed a method for quantifying indirect ictal frequency modulation in patients undergoing RNS treatment. To our knowledge, this is the first metric that quantifies a biomarker of the long-term efficacy of RNS. Given sufficiently many seizure patterns, this method demonstrated the potential to match qualitative expert assessments made using the same criteria as in Kokkinos *et al* (2019), and hence the potential to predict long-term clinical outcomes. Statistically significant fluctuations in the squared earth mover's metric of patients who did not show consistent indirect frequency modulation may indicate the direction in which RNS stimulation parameters must be tuned to produce this effect and improve seizure control. Quantification of indirect frequency modulation is but a first step in identifying and quantifying biomarkers of the long-term effects of RNS, as several other biomarkers have previously been identified and discussed qualitatively (Kokkinos *et al* 2019, Sisterson and Kokkinos 2020). Our quantification of frequency modulation may also be useful for tuning RNS stimulation parameters in a systematic feedback-driven manner, with the long-term goal of achieving genuinely personalized closed-loop brain modulation for epilepsy.

Data availability statement

The data that support the findings of this study are available upon reasonable request from the authors.

Acknowledgments

P V was supported in part by a Dowd Fellowship from the College of Engineering at Carnegie Mellon University, and in part by a Fellowship in Digital Health from the Center for Machine Learning and Health at Carnegie Mellon University. The authors would like to thank Philip and Marsha Dowd for their financial support and encouragement.

Conflicts of interest

R M R has served as a speaker for NeuroPace, Inc.

ORCID iDs

Praveen Venkatesh https://orcid.org/0000-0003-0752-1506
Pulkit Grover https://orcid.org/0000-0001-7651-7776
R Mark Richardson https://orcid.org/0000-0003-2620-7387
Vasileios Kokkinos https://orcid.org/0000-0002-4309-5455

References

Berg A T *et al* 2010 Revised terminology and concepts for organization of seizures and epilepsies: report of the ILAE commission on classification and terminology, 2005–2009 *Epilepsia* **51** 676–85

Bergey G K *et al* 2015 Long-term treatment with responsive brain stimulation in adults with refractory partial seizures *Neurology* **84** 810–7

Child N D, Stead M, Wirrell E C, Nickels K C, Wetjen N M, Lee K H and Klassen B T 2014 Chronic subthreshold subdural cortical stimulation for the treatment of focal epilepsy originating from eloquent cortex *Epilepsia* **55** e18–21

Elisevich K, Jenrow K, Schuh L and Smith B 2006 Long-term electrical stimulation-induced inhibition of partial epilepsy *J. Neurosurg.* **105** 894–7

Engel J Jr, van Ness P C, Rasmussen T B and Ojemann L M 1993 Outcome with respect to epileptic seizures *Surgical Treatment of the Epilepsies* ed J Engel Jr (New York: Raven Press) pp 609–21

Fisher R S *et al* 2017 Operational classification of seizure types by the International League Against Epilepsy: position paper of the ILAE commission for classification and terminology *Epilepsia* **58** 522–30

Fisher R S, Nune G, Roberts S E and Cramer J A 2015 The personal impact of epilepsy scale (PIES) *Epilepsy Behav.* **42** 140–6

Flamary R and Courty N 2017 POT: Python optimal transport library (available at: https://pythonot.github.io/)

Geller E B *et al* 2017 Brain-responsive neurostimulation in patients with medically intractable mesial temporal lobe epilepsy *Epilepsia* **58** 994–1004

Heck C N *et al* 2014 Two-year seizure reduction in adults with medically intractable partial onset epilepsy treated with responsive neurostimulation: final results of the RNS system pivotal trial *Epilepsia* **55** 432–41

Jobst B C *et al* 2017 Brain-responsive neurostimulation in patients with medically intractable seizures arising from eloquent and other neocortical areas *Epilepsia* **58** 1005–14

Kass R E, Eden U T and Brown E N 2014 *Analysis of Neural Data* (New York: Springer) (https://doi.org/10.1007/978-1-4614-9602-1)

Kerezoudis P, Grewal S S, Stead M, Lundstrom B N, Britton J W, Shin C, Cascino G D, Brinkmann B H, Worrell G A and van Gompel J J 2017 Chronic subthreshold cortical stimulation for adult drug-resistant focal epilepsy: safety, feasibility and technique *J. Neurosurg.* **129** 533–43

Kinoshita M *et al* 2004 Electric stimulation on human cortex suppresses fast cortical activity and epileptic spikes *Epilepsia* **45** 787–91

Kinoshita M *et al* 2005 Electric cortical stimulation suppresses epileptic and background activities in neocortical epilepsy and mesial temporal lobe epilepsy *Clin. Neurophysiol.* **116** 1291–9

Kokkinos V, Sisterson N D, Wozny T A and Richardson R M 2019 Association of closed-loop brain stimulation neurophysiological features with seizure control among patients with focal epilepsy *JAMA Neurol.* **76** 800–8

Kossoff E H, Ritzl E K, Politsky J M, Murro A M, Smith J R, Duckrow R B, Spencer D D and Bergey G K 2004 Effect of an external responsive neurostimulation on seizures and electrographic discharges during subdural electrode monitoring *Epilepsia* **45** 1560–7

Lesser R P, Kim S H, Beyderman L, Miglioretti D L, Webber W R, Bare M, Cysyk B, Krauss G and Gordon B 1999 Brief bursts of pulse stimulation terminate afterdischarges caused by cortical stimulation *Neurology* **53** 2073–81

Lundstrom B N, van Gompel J, Britton J, Nickels K, Wetjen N, Worrell G and Stead M 2016 Chronic subthreshold cortical stimulation to treat focal epilepsy *JAMA Neurol.* **73** 1370–2

Lundstrom B N, Worrell G A, Stead M and van Gompel J J 2017 Chronic subthreshold cortical stimulation: a therapeutic and potentially restorative therapy for focal epilepsy *Expert Rev. Neurother.* **17** 661–6

Mallat S 2009 Ch 11 covers denoising by thresholding *A Wavelet Tour of Signal Processing: The Sparse Way* 3rd edn (New York: Academic) (https://doi.org/10.1016/B978-0-12-374370-1.X0001-8)

Morrell M J and Halpern C 2016 Responsive direct brain stimulation for epilepsy *Neurosurg. Clin. North Am.* **27** 111–21

Nair D R *et al* 2020 Nine-year prospective efficacy and safety of brain-responsive neurostimulation for focal epilepsy *Neurology* **20** e1244–56

Osorio I, Frei M G, Sunderam S, Giftakis J, Bhavaraju N C, Schaffner S F and Wilkinson S B 2005 Automated seizure abatement in humans using electrical stimulation *Ann. Neurol.* **57** 258–68

Penfield W and Jasper H 1954 Electrocorticography *Epilepsy and the Functional Anatomy of the Human Brain* (Boston, MA: Little Brown) pp 692–738

Razavi B *et al* 2020 Real-world experience with direct brain-responsive neurostimulation for focal onset seizures *Epilepsia* **61** 1749–57

Sisterson N D and Kokkinos V 2020 Neuromodulation of epilepsy networks *Neurosurg. Clin. North Am.* **31** 459–70

Sisterson N D, Wozny T A, Kokkinos V, Bagic A, Urban A P, Richardson R M and Rational A 2020 Approach to understanding and evaluating responsive neurostimulation *Neuroinformatics* **18** 365–75

Sisterson N D, Wozny T A, Kokkinos V, Constantino A and Richardson R M 2019 Closed-loop brain stimulation for drug-resistant epilepsy: towards an evidence-based approach to personalized medicine *Neurotherapeutics* **16** 119–27

Skarpaas T L and Morrell M J 2009 Intracranial stimulation therapy for epilepsy *Neurotherapeutics* **6** 238–43

Stacey W C and Litt B 2008 Technology insight: neuroengineering and epilepsy—designing devices for seizure control *Nat. Clin. Pract. Neurol.* **4** 190–201

Thomas G P and Jobst B C 2015 Critical review of the responsive neurostimulator system for epilepsy *Med. Devices* **8** 405–11

Valentín A *et al* 2017 Intracranial stimulation for children with epilepsy *Eur. J. Paediatric Neurol.* **21** 223–31

Valentin A, Ughratdar I, Venkatachalam G, Williams R, Pina M, Lazaro M, Goyal S, Selway R and Alarcon G 2016 Sustained seizure control in a child with drug resistant epilepsy after subacute cortical electrical stimulation (SCES) *Brain Stimul.* **9** 307–9

Velasco A L, Velasco F, Velasco M, María Núñez J, Trejo D and García I 2009 Neuromodulation of epileptic foci in patients with non-lesional refractory motor epilepsy *Int. J. Neural Syst.* **19** 139–47

Velasco M, Velasco F, Velasco A L, Boleaga B, Jimenez F, Brito F and Marquez I 2000 Subacute electrical stimulation of the hippocampus blocks intractable temporal lobe seizures and paroxysmal EEG activities *Epilepsia* **41** 158–69

Villani C 2008 *Optimal Transport: Old and New* vol 338 (Berlin: Springer) (https://doi.org/10.1007/978-3-540-71050-9)

Virtanen P, Gommers R, Oliphant T E, Haberland M, Reddy T, Cournapeau D and van der Walt S J 2020 SciPy 1.0: fundamental algorithms for scientific computing in Python *Nat. Methods* **17** 261–72

Yamamoto J *et al* 2002 Low-frequency electric cortical stimulation has an inhibitory effect on epileptic focus in mesial temporal lobe epilepsy *Epilepsia* **43** 491–5

Yamamoto J *et al* 2006 Low-frequency electric cortical stimulation decreases interictal and ictal activity in human epilepsy *Seizure* **15** 520–7